Composite Structures 22 (1992) 3–13

Optimization for buckling resistance of fiber-composite laminate shells with and without cutouts

Hsuan-Teh Hu & Su Su Wang

National Center for Composite Materials Research, College of Engineering, University of Illinois, Urbana, Illinois 61801, USA

A sequential linear programming method with a simple move-limit strategy is used to investigate the following three important buckling optimization problems of composite shells: (1) optimization of fiber orientations for maximizing buckling resistance of composite shells without cutouts; (2) optimization of fiber orientations for maximizing buckling resistance of composite shells with circular cutouts; and (3) optimization of cutout geometry for maximizing buckling resistance of a composite shell. From the results of optimization study, it has been shown that, given a structural geometry, loading condition and material system, the buckling resistance of a cylindrical composite shell is strongly influenced by fiber orientations, end conditions, the presence of cutout and the geometry of cutout.

1 INTRODUCTION

Applications of fiber composite materials to advanced shell structures such as aircraft fuselages, deep submersibles and surface ships have increased rapidly in recent years. The fiber composite shell structures often contain complex layups and cutouts, as a result of practical needs. These composite laminate shells in service are commonly subjected to various kinds of external loading. Structural instability becomes a major concern in safe and reliable design of the advanced composite shells.

It is well known that buckling strength of fiber composite structures depends on various lamination parameters, such as ply orientations,[1–6] and geometric variables, such as structural configurations.[6–9] Therefore, proper selection of appropriate lamination and geometric variables for a given composite material system to realize its maximum structural buckling strength becomes a crucial problem. Also, reduction in buckling resistance of fiber composite structures because of the introduction of cutouts is of significant concern. The size, geometry and location of a cutout generally dictate the stability of the composite shell.[9–12] Consequently, the optimal configuration of a cutout in a fiber composite shell needs to be determined so that its structural buckling strength can be maximized.

Research on the subject of structural optimization has been reported by many investigators.[13] However, applications of optimization methods to stability analysis and design of complex fiber composite shell structures have been very limited. In this paper, a sequential linear programming method[14–16] is briefly reviewed in Section 2. This method and its associated algorithm are used to study the following important composite structural stability problems: (1) optimization of fiber orientations for maximizing buckling resistance of composite shells without cutouts; (2) optimization of fiber orientations for maximizing buckling resistance of composite shells with circular cutouts; and (3) optimization of cutout geometry for maximizing buckling resistance of a composite shell. Important conclusions obtained from the study are given in Section 4.

2 METHOD OF APPROACH

A general optimization problem may be defined as the following:

Minimize: $f(\mathbf{x})$ (1a)

Composite Structures 0263-8223/92/$05.00

Subject to: $g_i(\mathbf{x}) \le 0,\ i = 1,\ldots,r$ (1b)

$$h_j(\mathbf{x}) = 0,\ j = r+1,\ldots,m \quad (1c)$$

$$p_k \le x_k \le q_k,\ k = 1,\ldots,n \quad (1d)$$

where $f(\mathbf{x})$ is an objective function, $g_i(\mathbf{x})$ are inequality constraints, $h_j(\mathbf{x})$ are equality constraints, and $\mathbf{x} = \{x_1, x_2, \ldots, x_n\}^T$ is a vector of design variables. Any function f which satisfies the above constraints is called an admissible function. The set of all admissible functions is called the admissible space. If a particular optimization problem requires maximization, we simply minimize $-f(\mathbf{x})$.

2.1 Linearization

The basic concept of a sequential linear programming is that, given a feasible solution $\mathbf{x}_0 = \{x_{01}, x_{02}, \ldots, x_{0n}\}^T$ for an optimization problem, a linear programming method may be established by expanding the nonlinear functions about $\mathbf{x}_0$ in a Taylor series, and ignoring terms of order higher than the linear ones in the expansion. With this approximation, the optimization problem, eqns (1a)–(1d), becomes

Minimize: $f(\mathbf{x}) \approx f(\mathbf{x}_0) + \nabla f(\mathbf{x}_0)^T \delta\mathbf{x}$ (2a)

Subject to: $g_i(\mathbf{x}) \approx g_i(\mathbf{x}_0) + \nabla g_i(\mathbf{x}_0)^T \delta\mathbf{x} \le 0$ (2b)

$$h_j(\mathbf{x}) \approx h_j(\mathbf{x}_0) + \nabla h_j(\mathbf{x}_0)^T \delta\mathbf{x} = 0 \quad (2c)$$

$$p_k \le x_k \le q_k \quad (2d)$$

where $i = 1,\ldots,r$; $j = r+1,\ldots,m$; $k = 1,\ldots,n$; $\delta\mathbf{x} = \{x_1 - x_{01}, x_2 - x_{02}, \ldots, x_n - x_{0n}\}^T$.

It is clear that eqns (2a)–(2d) represent a linear programming problem where variables are contained in the vector space $\delta\mathbf{x}$. The functions $f(\mathbf{x}_0)$, $g_i(\mathbf{x}_0)$ and $h_j(\mathbf{x}_0)$ and their gradients $\nabla f(\mathbf{x}_0)$, $\nabla g_i(\mathbf{x}_0)$ and $\nabla h_j(\mathbf{x}_0)$ are all constants. A solution for eqns (2a)–(2d) may be easily obtained by the Simplex method.[17] After obtaining an initial approximate solution for eqns (2a)–(2d), say $\mathbf{x}_1$, we can linearize the original problem, eqns (1a)–(1d), at $\mathbf{x}_1$ and solve the new linear programming problem. The process is repeated until a convergent solution is obtained.

2.2 Move limit

Although the procedure for a sequential linear programming is simple, difficulties may arise during the iterations. First, the optimum solution for the approximate linear problem may violate the constraint conditions of the original optimization problem. Second, in a nonlinear problem, the true optimum solution may appear between two constraint intersections. A straightforward successive linearization in such a case may lead to an oscillation of the solution between the widely separated values. Difficulties in dealing with such a problem may be avoided by imposing a 'move limit' on the linear approximation.[14-16]

The concept of a move limit is that a set of box-like admissible constraints are placed in the range of $\delta\mathbf{x}$. It is known that computational economy and accuracy of the approximate solution may depend greatly on the choice of the move limit. (If the move limits are made too small, solution convergence may be very slow. If they are too large, oscillations may occur.) In general, the choice of a suitable move limit depends on experience and also on the results of previous steps. Once a proper move limit is chosen at the beginning of the sequential linear programming procedure, this move limit should gradually approach zero as the iterative process continues.[14,16,18]

2.3 Numerical algorithm

The algorithm of a sequential linear programming with selected move limits may be summarized as follows:

(1) Linearize the nonlinear objective function and associated constraints with respect to an initial guess $\mathbf{x}_0$.
(2) Impose move limits in the form of $-\mathbf{L} \le (\mathbf{x} - \mathbf{x}_0) \le \mathbf{U}$, where $\mathbf{L}$ and $\mathbf{U}$ are properly chosen positive constraints, which approach zero gradually, when the iteration number in the sequential linear programming process becomes large.
(3) Solve the approximate linear programming problem to obtain an initial optimum solution $\mathbf{x}_1$.
(4) Repeat the process by redefining $\mathbf{x}_1$ with $\mathbf{x}_0$ until either the subsequent solutions do not change significantly (i.e. true convergence) or the move limit approaches zero (i.e. forced convergence).

3 OPTIMIZATION FOR COMPOSITE SHELL BUCKLING

The sequential linear programming method described above is used to conduct various optimization studies on buckling resistance of

fiber composite laminate cylindrical shells with and without cutouts, which are subjected to external hydrostatic loading. The composite laminate shells analyzed in the following sections all have the same structural geometry and ply constitutive properties. The composite shells have similar ply layups, i.e. $[\pm\theta/90_2/0]_{10S}$, and are subjected to external hydrostatic compression. In the present study, the objective function for all the problems is the critical buckling pressure p_{cr}. Also, separate buckling analyses of the composite shells in the first two problems are carried out for the purposes of comparison and verification of solution accuracy.

3.1 Optimization of fiber orientations for fiber composite shells without cutouts

In this problem, fiber composite laminate cylindrical shells (Fig. 1) with three different end conditions, i.e. fixed, simply supported, and free ends, are investigated. In all of these cases, the shells do not contain any cutouts ($d=0$). The objective is to determine the optimal fiber angle θ to maximize the buckling resistant pressure p_{cr} of the composite laminate shell in each case studied.

Based on the sequential linear programming method, in each iteration the current, linearized optimization problem becomes

$$\text{Maximize:}\quad p_{cr}(\theta)\approx p_{cr}(\theta_0)+(\theta-\theta_0)\left.\frac{\partial p_{cr}}{\partial\theta}\right|_{\theta=\theta_0} \tag{3a}$$

$$\text{Subject to:}\quad 0°\le\theta\le 90° \tag{3b}$$

$$|(\theta-\theta_0)|\le r\times q\times 0{\cdot}5^s \tag{3c}$$

where θ_0 is a solution in the current iteration, and r and q in eqn (3c) are size and reduction rate of move limit. In the present study, the values of r and q are selected to be 18° and $0{\cdot}8^{(N-1)}$, where N is a current iteration number. To minimize the oscillation of the solution, a tolerance-limit parameter $0{\cdot}5^S$ is introduced in the move limit, where s is the number of oscillations of the derivative $\partial p_{cr}/\partial\theta$ that have taken place before the current iteration. The value of s increases by one if the sign of $\partial p_{cr}/\partial\theta$ changes. The use of this parameter is similar to that in the bisection method.[19] Whenever oscillation of the solution occurs, the range of the move limit is reduced to half of its current value. This increases the solution convergent rate considerably.

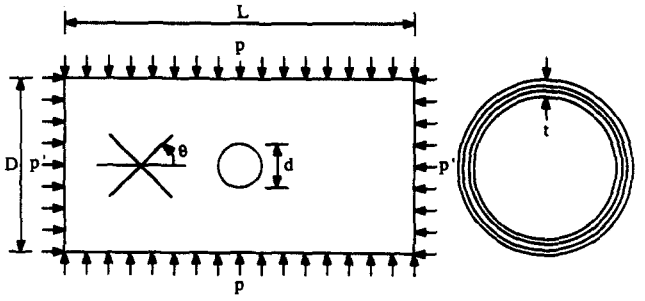

Laminate layup:
$[\pm\theta/90_2/0]_{10S}$

Composite shell geometry:
L = 40.64 cm. (16 in.)
D = 20.32 cm. (8 in.)
t = 1.27 cm. (0.5 in.)

Cutout geometry (circular hole):
d = 5.08 cm. (2 in.)

Ply constitutive properties:
E_{11} = 138000 MPa
E_{22} = 14500 MPa
$G_{12}=G_{13}$ = 5870 MPa
G_{23} = 3520 MPa
ν_{12} = 0.21

Loading:
p' = 3.75 p

Fig. 1. Cylindrical composite laminate shell with circular cutout.

To evaluate the buckling pressure $p_{cr}(\theta_0)$ of the composite laminate shell, the ABAQUS finite-element program[20] is used for the linearized buckling problem. In the present analysis, the structure is modeled by eight-node, isoparametric laminate shell elements.

We remark that the derivative $\partial p_{cr}/\partial\theta$ in eqn (3a) may be approximated by using a forward finite-difference method with the following form:

$$\frac{\partial p_{cr}}{\partial\theta}\approx\frac{[p_{cr}(\theta_0+\Delta\theta)-p_{cr}(\theta_0)]}{\Delta\theta} \tag{4}$$

To determine the value of $\partial p_{cr}/\partial\theta$ in eqn (4) numerically, two incremental analyses are needed to compute $p_{cr}(\theta_0)$ and $p_{cr}(\theta_0+\Delta\theta)$ in each iteration. In this example, the value of $\Delta\theta$ is selected to be 1° in most iterations.

Some of the important numerical results obtained are given in Fig. 2. The initial values of θ are selected to be 0° for the $[\pm\theta/90_2/0]_{10S}$ shells with fixed ends and with simply supported ends, and 10° for the shell with free ends. The buckling pressure p_{cr} associated with each $\Delta\theta$ is determined in the iteration. After 11 iterations, the optimal value of θ converges to 50·4° for the shell with fixed ends, 47·5° with simply supported ends, and 90° with free ends. Buckling modes of these shells associated with the first iteration and the converged final (optimal) solutions are given in Figs 3–5.

In a separate bifurcation study, critical pressures p_{cr} are determined as a function of θ for the $[\pm\theta/90_2/0]_{10S}$ composite laminate shells with the three end conditions described above. The

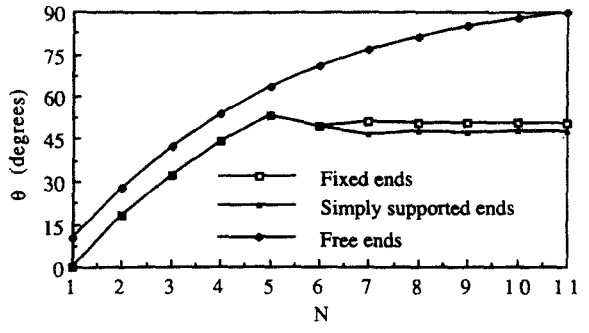

(a)

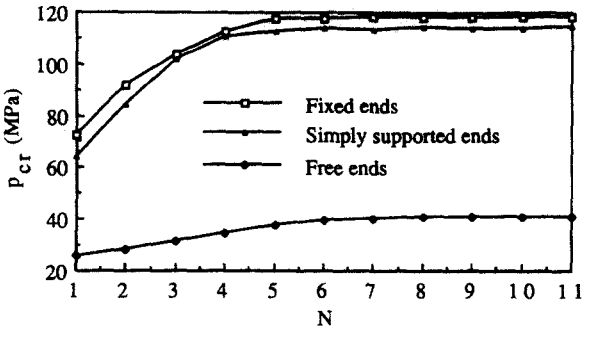

(b)

Fig. 2. Buckling optimization of $[\pm\theta/90_2/0]_{10S}$ composite laminate shells without cutout subjected to hydrostatic compression. (a) Number of iterations N versus fiber orientation θ; (b) number of iterations N versus critical pressure p_{cr}.

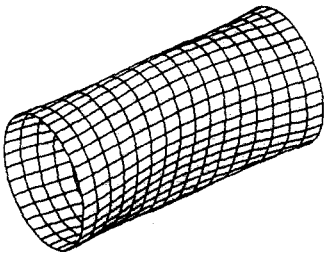

Lowest buckling mode of the initial solution (iteration 1, θ = 0°)

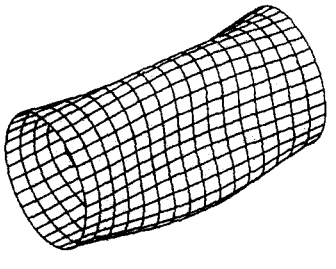

Lowest buckling mode of the optimal solution (iteration 11, θ = 50.4°)

Fig. 3. Buckling modes of $[\pm\theta/90_2/0]_{10S}$ composite laminate shells without cutout subjected to hydrostatic compression (fixed ends).

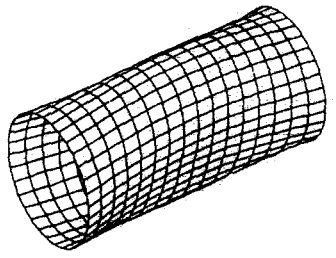

Lowest buckling mode of the initial solution (iteration 1, θ = 0°)

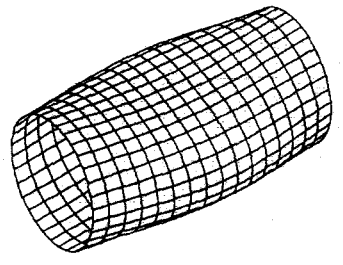

Lowest buckling mode of the optimal solution (iteration 11, θ = 47.5°)

Fig. 4. Buckling modes of $[\pm\theta/90_2/0]_{10S}$ composite laminate shells without cutout subjected to hydrostatic compression (simply supported ends).

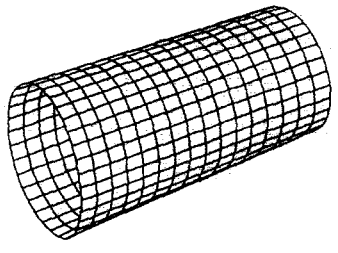

Lowest buckling mode of the initial solution (iteration 1, θ = 10°)

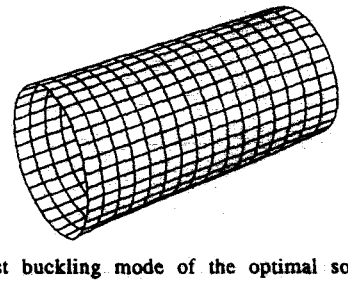

Lowest buckling mode of the optimal solution (iteration 11, θ = 90°)

Fig. 5. Buckling modes of $[\pm\theta/90_2/0]_{10S}$ composite laminate shells without cutout subjected to hydrostatic compression (free ends).

angles θ corresponding to the maximum critical pressure (Fig. 6) are consistent with the present optimization solutions, i.e. $\theta \approx 50{\cdot}4°$ for the case with fixed ends, $\theta \approx 47{\cdot}5°$ with simply supported ends and $\theta \approx 90°$ with free ends. This demonstrates the accuracy and the validity of the sequential linear programming.

From the numerical results it can be seen that critical buckling pressure p_{cr} for a cylindrical

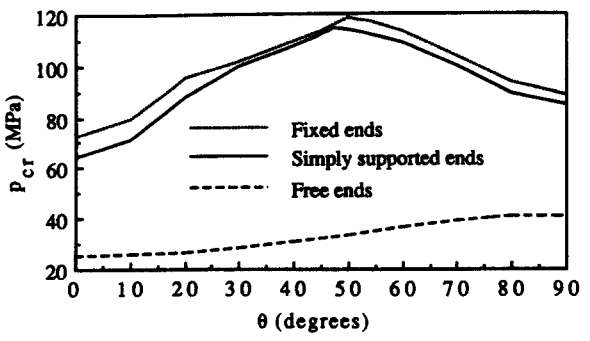

Fig. 6. Critical pressure p_{cr} as a function of θ for $[\pm\theta/90_2/0]_{10S}$ composite laminate shells without cutout subjected to hydrostatic compression.

composite shell is strongly influenced by fiber orientations as well as end conditions. Given optimal fiber orientations, the values of p_{cr} for $[\pm\theta/90_2/0]_{10S}$ composite shells with fixed ends and with simply supported ends are much greater than that for the same shell with free ends.

3.2 Optimization of fiber orientations for composite shells with circular cutouts

In the second example, the effect of fiber orientations on the buckling resistance of a fiber composite laminate shell containing a cutout is studied. For comparison, composite shells with the same geometric, material, lamination variables, end and loading conditions as those studied in Section 3.1 are considered. Circular cutouts with $d = 5{\cdot}08$ cm (2 in) are located at the center of the mid-spans of the composite shells (Fig. 1). With the above objectives in mind, the optimal fiber angles $\pm\theta$ are determined to maximize the critical buckling pressure p_{cr} of the composite laminate shells containing circular cutouts with different end conditions.

The linearized optimization problem can be posited in exactly the same way as the first example given in Section 3.1. Again, the shells are modeled with eight-node isoparametric shell elements and analyzed with the ABAQUS program.

Numerical results of the buckling optimization study of the composite laminate shells with cutouts are given in Fig. 7. The initial values of θ selected for optimization are 0° for the $[°\theta/90_2/0]_{10S}$ shells with fixed ends and with simply supported ends, and 10° for the shell with free ends. The buckling pressure p_{cr} associated with each $\Delta\theta$ in the iteration process is determined. The optimal value of θ converges to 53·1° for the shell with fixed ends after nine iterations. (Although iterations 10 and 11 were carried out, their solutions were very close to the solution of iteration 9.) After 11 iterations, the optimal value of θ converges to 51·4° for the shell with simply supported ends, and 90° for the shell with free ends. Buckling modes of these shells associated with the first iteration and the final (optimal) solutions are shown in Figs 8–10.

Again, in a separate bifurcation study, the critical pressure p_{cr} is determined as a function of θ for the $[\pm\theta/90_2/0]_{10S}$ composite laminate shells with circular cutouts and with different end conditions. The angles θ corresponding to the maximum critical pressure (Fig. 11) are consistent with the above numerical optimal solutions. These results demonstrate again the validity and accuracy of the sequential linear programming.

From the numerical results obtained, one can see that the critical buckling pressure p_{cr} for the cylindrical composite shell with a circular cutout is strongly influenced by the end conditions as well as fiber orientations. Given the optimal fiber orientations, the values of p_{cr} for the $[\pm\theta/90_2/0]_{10S}$ composite shells with fixed ends and with simply supported ends are much greater than that for the same shell with free ends.

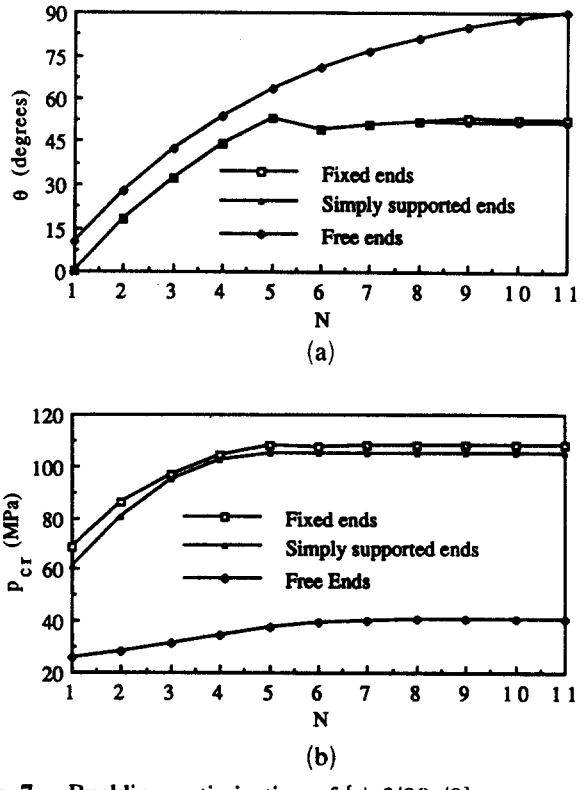

Fig. 7. Buckling optimization of $[\pm\theta/90_2/0]_{10S}$ composite laminate shells with circular cutouts subjected to hydrostatic compression. (a) Number of iterations N versus fiber orientation θ; (b) number of iterations N versus critical pressure p_{cr}.

Comparing the solutions for optimal fiber angles ($\pm\theta$) of the shells containing cutouts with those for the previous examples in Section 3.1 (i.e. shells without cutouts), one can clearly see that they converge to different values for the cases with fixed ends (53·1° versus 50·4° in Fig. 12(a)) and for the cases with simply supported ends (51·4° versus 47·5° in Fig. 13(a)). However, for the shells with free ends the optimal fiber angles converge to the same value (90°) whether a cutout is present or not (Fig. 14(a)). Therefore, it can be concluded that the optimal fiber angle θ is sensitive to the presence of cutouts in $[\pm\theta/90_2/0]_{10S}$ composite shells with fixed ends and with simply supported ends, but not for the composite shells with free ends.

Finally, comparing the critical buckling pressures p_{cr} obtained for the examples in this section with those in Section 3.1, one can see that for the composite shells with fixed ends and with simply supported ends, the cases with a circular cutout experience appreciable reductions in the

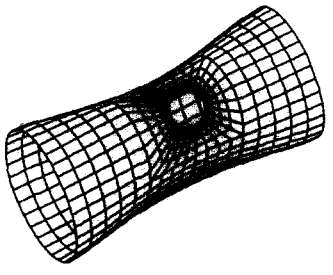

Lowest buckling mode of the initial solution (iteration 1, θ = 0°)

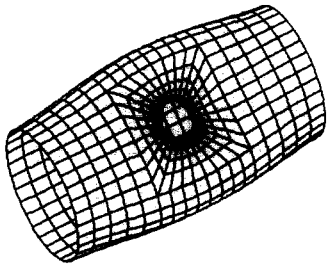

Lowest buckling mode of the optimal solution (iteration 9, θ = 53.1°)

Fig. 8. Buckling modes of $[\pm\theta/90_2/0]_{10S}$ composite laminate shells with circular cutouts subjected to hydrostatic compression (fixed ends).

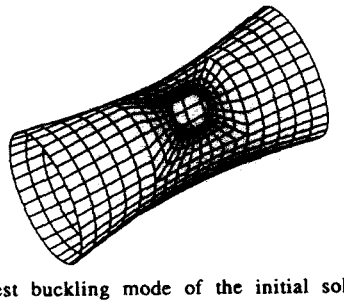

Lowest buckling mode of the initial solution (iteration 1, θ = 0°)

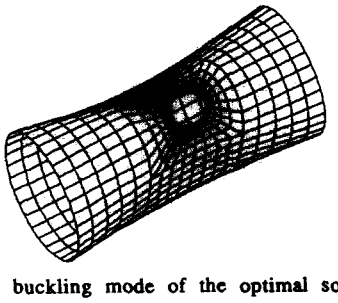

Lowest buckling mode of the optimal solution (iteration 11, θ = 51.4°)

Fig. 9. Buckling modes of $[\pm\theta/90_2/0]_{10S}$ composite laminate shells with circular cutouts subjected to hydrostatic compression (simply supported ends).

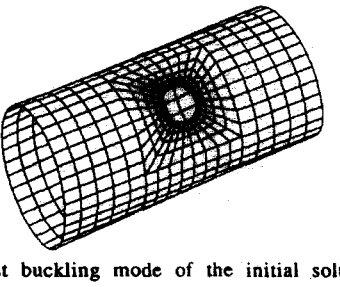

Lowest buckling mode of the initial solution (iteration 1, θ = 10°)

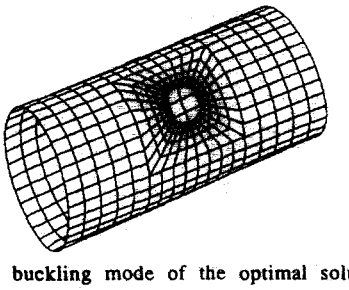

Lowest buckling mode of the optimal solution (iteration 11, θ = 90°)

Fig. 10. Buckling modes of $[\pm\theta/90_2/0]_{10S}$ composite laminate shells with circular cutouts subjected to hydrostatic compression (free ends).

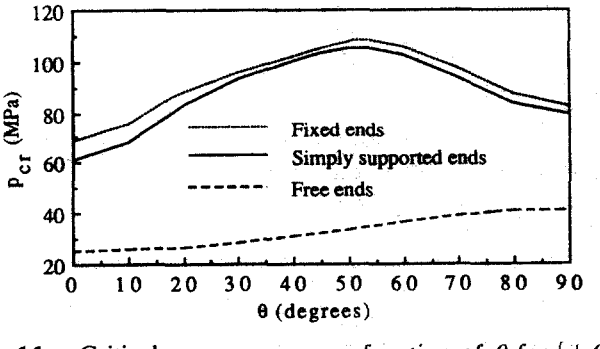

Fig. 11. Critical pressure p_{cr} as a function of θ for $[\pm\theta/90_2/0]_{10S}$ composite laminate shells with circular cutouts subjected to hydrostatic compression.

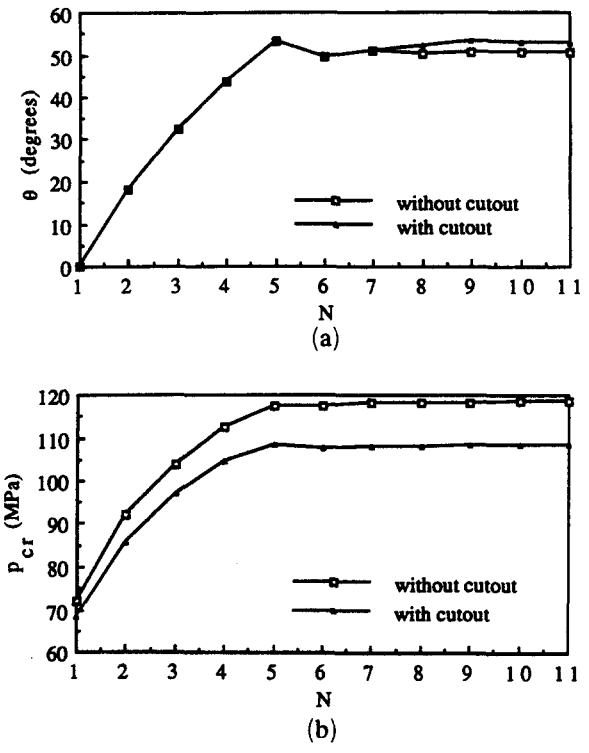

Fig. 12. Buckling optimization of $[\pm\theta/90_2/0]_{10S}$ composite laminate shells subjected to hydrostatic compression (fixed ends). (a) Number of iterations N versus fiber orientation θ; (b) number of iterations N versus critical pressure p_{cr}.

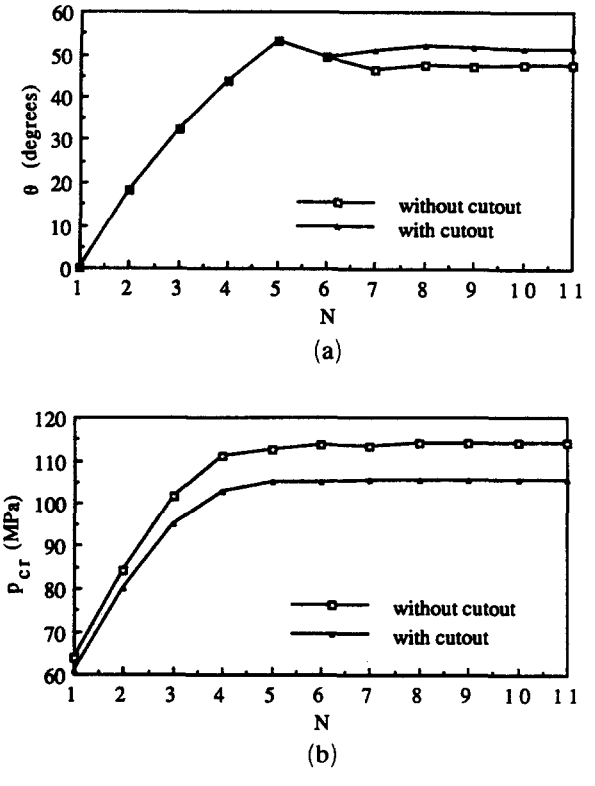

Fig. 13. Buckling optimization of $[\pm\theta/90_2/0]_{10S}$ composite laminate shells subjected to hydrostatic compression (simply supported ends). (a) Number of iterations N versus fiber orientation θ; (b) number of iterations N versus critical pressure p_{cr}.

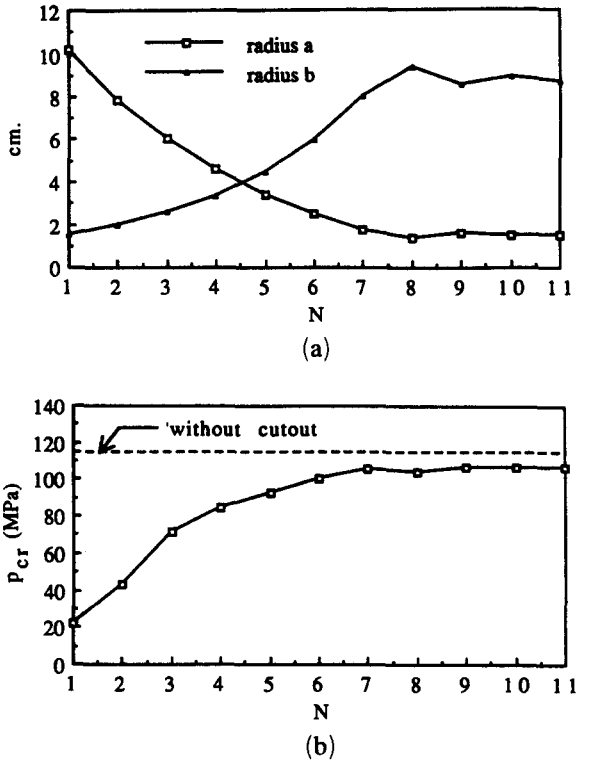

Fig. 14. Buckling optimization of $[\pm\theta/90_2/0]_{10S}$ composite laminate shells subjected to hydrostatic compression (free ends). (a) Number of iterations N versus fiber orientation θ; (b) number of iterations N versus critical pressure p_{cr}.

critical pressure (Figs 12(b) and 13(b)). However, for the composite shell with free ends, the circular cutout has almost no influence on the buckling pressure (Fig. 14(b)).

3.3 Optimization of cutout geometry for fiber composite shell

We now consider a simply supported fiber-composite laminate shell with the same geometry, lamination layup, ply constitutive properties and loading condition as those studied in previous sections. However, this shell contains an elliptic cutout, with radii a and b, at the center of the mid-span (Fig. 15). Based on the solutions obtained in Section 3.1, the optimal fiber orientations $[\pm 47{\cdot}5/90_2/0]_{10S}$ are chosen in the present study. The objective here is to determine the optimal geometry (i.e. a and b) of the elliptic cutout so that the buckling pressure p_{cr} of the shell can be maximized.

A constraint condition that the curved surface area A^* of the cutout is constant (say, $1/\alpha$ of the total surface area A of the shell) is introduced for practical considerations. The surface area A^* of

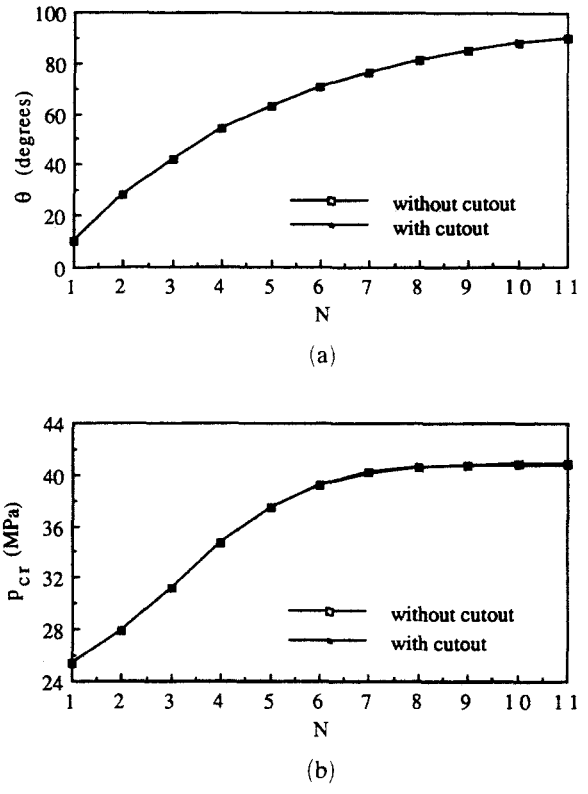

Fig. 15. Cylindrical composite laminate shell with elliptic cutout.

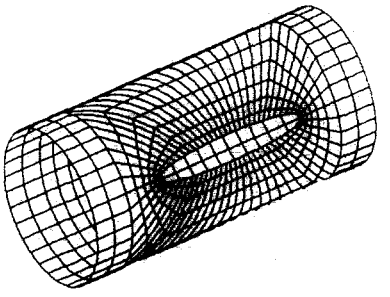

Initial cutout shape
a = 10.16 cm. (4.0 in.) and b = 1.52 cm. (0.6 in.)

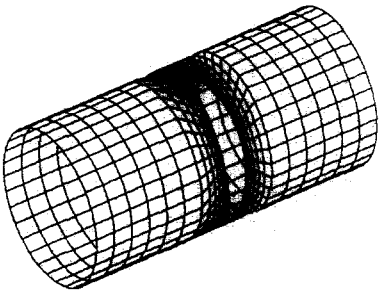

Final optimal cutout shape
a = 1.52 cm. (0.6 in.) and b = 8.69 cm. (3.42 in.)

Fig. 17. Initial guess and final optimal configurations of the cutout in $[\pm 47{\cdot}5/90_2/0]_{10S}$ composite shells with simply supported ends subjected to hydrostatic compression.

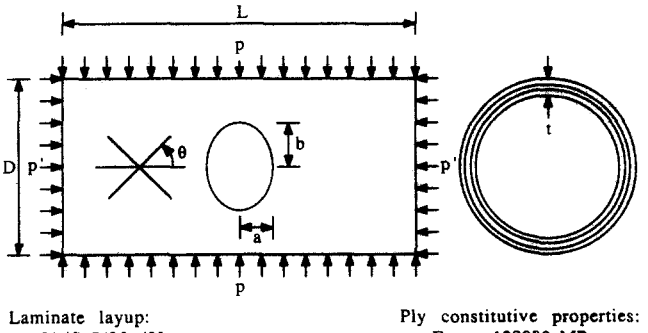

Laminate layup:
$[\pm 47.5/90_2/0]_{10S}$

Composite shell geometry:
L = 40.64 cm. (16 in.)
D = 20.32 cm. (8 in.)
t = 1.27 cm. (0.5 in.)

Cutout geometry (elliptic hole, radii a & b):
A*/A = 1/α

Ply constitutive properties:
E_{11} = 138000 MPa
E_{22} = 14500 MPa
$G_{12} = G_{13}$ = 5870 MPa
G_{23} = 3520 MPa
ν_{12} = 0.21

Loading:
p' = 3.75 p

Fig. 16. Buckling optimization of $[\pm 47{\cdot}5/90_2/0]_{10S}$ composite laminate shells with elliptic cutouts subjected to hydrostatic compression (simply supported ends). (a) Number of iterations N versus radii a and b; (b) number of iterations N versus critical pressure p_{cr}.

the cutout can be shown (Ref. 21) as

$$A^* = 2D\int_0^a \sin^{-1}\left[\frac{2b}{D}\sqrt{\left(1-\frac{z^2}{a^2}\right)}\right]\mathrm{d}z \qquad (5)$$

This constraint condition can be rewritten as $A^* = A/\alpha$, or

$$2D\int_0^a \sin^{-1}\left[\frac{2b}{D}\sqrt{\left(1-\frac{z^2}{a^2}\right)}\right]\mathrm{d}z = \pi DL/\alpha \qquad (6)$$

In this study, α is selected as 50 for illustrative purposes. The constraint reduces the number of independent geometric parameters from two to one. The constraint equation can be solved numerically, and an explicit relationship between a and b is given in Ref. 21.

In the sequential linear programming analysis, for each iteration the linearized optimization problem becomes

$$\text{Maximize:} \quad p_{cr}(a) \approx p_{cr}(a_0) + (a-a_0)\left.\frac{\partial p_{cr}}{\partial a}\right|_{a=a_0} \qquad (7a)$$

$$\text{Subject to:} \quad 0 \le a \le L/2 \qquad (7b)$$

$$0 \le b \le D/2 \qquad (7c)$$

$$|(a-a_0)| \le r \times q \times 0{\cdot}5^s \qquad (7d)$$

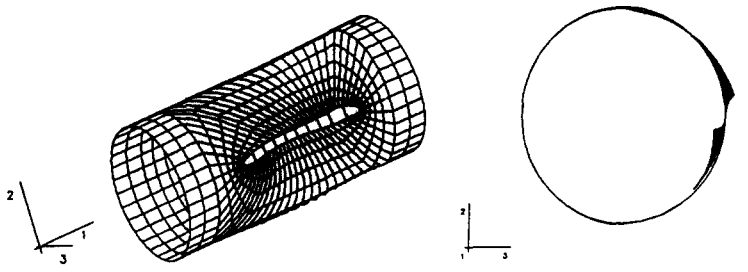

First buckling mode for shell with initially elliptic cutout
a = 10.16 cm. (4.0 in.), b = 1.52 cm. (0.6 in.), p_{cr} = 22.0 MPa

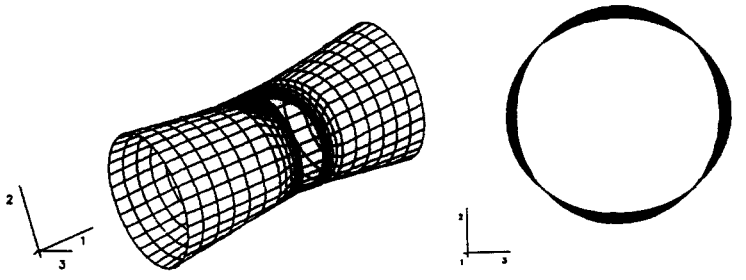

First buckling mode for shell with optimal elliptic cutout
a = 1.52 cm. (0.6 in.), b = 8.69 cm. (3.42 in.), p_{cr} = 106.3 MPa

Fig. 18. Buckling modes of $[\pm 47{\cdot}5/90_2/0]_{10S}$ composite laminate shell containing elliptic cutout with initial and optimal configurations (simply supported ends, subjected to hydrostatic compression).

where a_0 is the current solution. The size r and the reduction rate q of the move limit are selected to be 2·29 cm (0·9 in) and $0{\cdot}8^{(N-1)}$, respectively.

The derivative $\partial p_{cr}/\partial a$ in eqn (7a) can be evaluated in the same manner as that in eqn (4), with θ being replaced by a. To calculate $\partial p_{cr}/\partial a$, incremental analyses are needed to compute $p_{cr}(a_0)$ and $p_{cr}(a_0+\Delta a)$ in each iteration. In the present study, the value of Δa is selected to be 0·13 cm (0·05 in) in most iterations.

Some of the key results obtained in the optimization study are given in Fig. 16. The initial guess introduced is $a = 10{\cdot}16$ cm (4·0 in) and $b = 1{\cdot}52$ cm (0·6 in). The final solution converges to $a = 1{\cdot}52$ cm (0·6 in) and $b = 8{\cdot}69$ cm (3·42 in). The initial guess and the final optimal configuration of the cutout are shown in Fig. 17. The first buckling modes of the shells with initial and final (optimal) cutout geometry are shown in Fig. 18.

From Fig. 16, it can be seen that when the major radius of the elliptic cutout is normal to the hoop direction, i.e. $a > b$, the buckling resistance of the composite shell tends to be low. The longer a is, the lower p_{cr} becomes. On the other hand, when the major radius of the elliptic cutout is parallel to the hoop direction, i.e. $a < b$, the buckling resistance of the composite shell tends to be high. The longer b is, the higher p_{cr} becomes. The buckling pressure for the case of an elliptic cutout with its major axis parallel to the hoop direction (i.e. the final optimal configuration) is 4·8 times higher than that with the cutout in an orthogonal position (i.e. the initial guess configuration). These results are not unexpected, as the ratio of the hoop stress to axial stress is 2/1 for a cylindrical shell under hydrostatic loading without the cutout. The major radius of the elliptic cutout tends to be parallel to the hoop direction (i.e. the high stress direction) to achieve the maximum buckling resistance. Although the optimal solution for b is 8·69 cm (3·42 in), not equal to the shell radius 9·53 cm (3·75 in), it is close to this extreme case.

When the buckling mode of the composite shell containing a cutout with the initially assumed configuration is compared with that of the composite shell with the final (optimal) cutout geometry (Fig. 18), it can be clearly seen that buckling mode shape in the former case is local around the cutout. However, in the latter case, mode shape is global for the entire composite structure. Therefore, for the simply supported fiber composite laminate shell with an elliptic cutout, we conclude that when the radius a is much greater than the radius b, the governing buckling mode is local whereas in the case of the radius b being much

greater than the radius a, the governing buckling mode is global.

4 CONCLUSIONS

From the results obtained in this study, the following conclusions can be drawn:

(1) Given a structural geometry, loading condition and material system, the buckling resistance of a cylindrical composite shell is strongly influenced by fiber orientations, end conditions and the presence of a circular cutout.

(2) For the $[\pm\theta/90_2/0]_{10S}$ composite shell systems with fixed ends and with simply supported ends, the optimal fiber angle θ for maximum buckling resistance under external hydrostatic compression is sensitive to the presence of a circular cutout, but is not for shells with free ends.

(3) For the $[\pm\theta/90_2/0]_{10S}$ composite shells with fixed ends and with simply supported ends under external hydrostatic compression, appreciable reductions in the critical pressure are experienced in the cases with a circular cutout. However, for the same composite shells with free ends, the circular cutout has almost no influence on the buckling pressure.

(4) Given the optimal fiber orientations in a composite laminate shell containing an elliptic cutout of a constant area, the buckling resistance of the shell is governed by the geometry of the cutout. For example, in a simply supported, cylindrical composite shell with a $[\pm 47{\cdot}5/90_2/0]_{10S}$ layup, the optimal configuration of the elliptic cutout is found to have its major axis parallel to the hoop direction. The buckling pressure for the case of an elliptic cutout with its major axis parallel to the hoop direction is 4·8 times higher than that with the cutout in an orthogonal position.

(5) For a simply supported $[\pm 47{\cdot}5/90_2/0]_{10S}$ cylindrical composite shell, when the major axis of the elliptic cutout is along the axial direction with its radius much greater than that along the hoop direction, the governing buckling mode is local. However, when the major axis of the elliptic cutout is along the hoop direction with its radius much greater than that along the axial direction, the governing buckling mode is global.

ACKNOWLEDGEMENTS

The work reported in this paper was supported in part by grants from CONOCO, Inc., and by the Office of Naval Research (ONR) through the University Research Initiative Program (Grant N00014-86-K-0799) to the National Center for Composite Materials Research (NCCMR) at the University of Illinois at Urbana–Champaign, Illinois. Computation in this research was carried out in the Digital Computer Laboratory at NCCMR. The authors are grateful to Professor B. P. Wang of the University of Texas at Arlington for fruitful discussion in the early stage of the research. The authors are also indebted to Dr R. F. Jones of ONR Mechanics Division and to Drs J. G. Williams and M. M. Salama of CONOCO, Inc., for their encouragement and support during the course of this study.

REFERENCES

1. Hirano, Y., Buckling of angle-ply laminated circular cylindrical shells. *Journal of Applied Mechanics, ASME*, **46** (1979) 233–4.
2. Nshanian, Y. S. & Pappas, M., Optimal laminated composite shells for buckling and vibration. *AIAA Journal*, **21** (3) (1983) 430–7.
3. Onoda, J., Optimal laminate configurations of cylindrical shells for axial buckling. *AIAA Journal*, **23** (7) (1985) 1093–8.
4. Sun, G. & Hansen, J. S., Optimal design of laminated-composite circular-cylindrical shells subjected to combined loads. *Journal of Applied Mechanics, ASME*, **55** (1) (1988) 136–42.
5. Muc, A., Optimal fibre orientation for simply-supported, angle-ply plates under biaxial compression. *Composite Structures*, **9** (1988) 161–72.
6. Jun, S. M. & Hong, C. S., Buckling behavior of laminated composite cylindrical panels under axial compression. *Computers and Structures*, **29** (3) (1988) 479–90.
7. Whitney, J. M., Buckling of anisotropic laminated cylindrical plates. *AIAA Journal*, **22** (11) (1984) 1641–5.
8. Leissa, A. W., *Buckling of Laminated Composite Plates and Shell Panels*. AFWAL-TR-85-3069. Flight Dynamics Laboratory, Air Force Wright Aeronautical Laboratories, Wright-Patterson AFB, OH, 1985, Chapter X.
9. Knight, N. F. & Starnes, J. H., Postbuckling behavior of axially compressed graphite–epoxy cylindrical panels with circular holes. *Journal of Pressure Vessel Technology, ASME*, **107** (4) (1985) 394–402.
10. Starnes, J. H. & Rouse, M., Postbuckling and failure characteristics of selected flat rectangular graphite–epoxy plates loaded in compression. In *Proceedings of the 22nd AIAA/ASME/ASCE/AHS Structures, Structural Dynamics and Materials Conference, (AIAA CP 811)*, 1981, pp. 423–34.
11. Larsson, P.-L., On buckling of orthotropic compressed plates with circular holes. *Composite Structures*, **7** (2) (1987) 103–21.

12. Nemeth, M. P., Buckling behavior of compression-loaded symmetrically laminated angle-ply plates with holes. *AIAA Journal*, **26** (3) (1988) 330–6.
13. Schmit, L. A., Structural synthesis — its genesis and development. *AIAA Journal*, **19** (10) (1981) 1249–63.
14. Vanderplaats, G. N., *Numerical Optimization Techniques for Engineering Design with Applications*. McGraw-Hill, New York, 1984, Chapter 6.
15. Haftka, R. T. & Kamat, M. P., *Elements of Structural Optimization*. Martinus Nijhoff, Dordrecht, 1985, Chapter 3.
16. Zienkiewicz, O. C. & Champbell, J. S., Shape optimization and sequential linear programming. In *Optimum Structural Design, Theory and Applications*, ed. R. H. Gallagher, O. C. Zienkiewicz. Wiley, New York, 1973, pp. 109–26.
17. Kolman, B. & Beck, R. E., *Elementary Linear Programming with Applications*. Academic Press, Orlando, FL, 1980, Chapter 2.
18. Esping, B. J. D., Minimum weight design of membrane structures. *Computers and Structures*, **19** (5/6) (1984) 707–16.
19. Maror, M. J., *Numerical Analysis, A Practical Approach*, 2nd edn. Macmillan, New York, 1987, Chapter 2.
20. Anonymous, *ABAQUS User Manual*, Version 4-7. Hibbitt, Karlsson & Sorensen, Providence, RI, 1989.
21. Hu, H.-T. & Wang, S. S., Optimization for buckling resistance of fiber-composite laminate shells with and without cutouts. In *Proceedings of the 31st AIAA/ASME/ASCE/AHS/ASC Structures, Structural Dynamics and Materials Conference, (AIAA paper 90-1069)*, Long Beach, CA, 2–4 April 1990; also Technical Report UIUC-NCCMR-89-25, National Center for Composite Materials Research, University of Illinois, Urbana, 1989.